

**THE PRECIPITATION OF IRON IN EARLY SMELTED COPPER FROM TIMNA**

J. F. Roeder, J. F. Sculac, and M. R. Notis

The archaeological site at Timna in the Aravah Region of Southern Israel is one of the most important sites relevant to the beginnings of metallurgical practice. First, it is a site where complete furnaces, tuyeres, slags, ores, and copper ingots have been found in situ<sup>1</sup> and representing different stages in metallurgical development, dating as early as the Chalcolithic Period (4th millenium B.C.). Second, because of the nature of the iron content of the copper ingots<sup>2</sup> and some of the unique iron artifacts which have been found,<sup>3</sup> it may be the strongest evidence that demonstrates that early iron smelting and metallurgy developed directly from copper metallurgy. For this study, a small piece of a copper ingot found at the site identified as Timna Site 2 (sample no. 575) was provided by Beno Rothenberg, the director of the excavations at Timna.

Three morphological forms have been reported in the literature for the iron-rich phases found in high copper-iron alloys: (1) a primary iron phase originating during solidification, and often dendritic in form;<sup>1,2,4</sup> (2) small spherical coherent solid-state precipitates;<sup>5-14</sup> and (3) intermediate-size star-shaped or cuboid precipitates.<sup>4,8,9,14</sup>

Milton et al.<sup>2</sup> noted that copper from Timna was strongly magnetic and then confirmed the presence of metallic iron by metallographic examination. Later work,<sup>1</sup> with copper samples taken from modern simulation smelting experiments thought to have been performed under similar conditions to those used at Timna, showed the presence of randomly oriented dendritic iron in the copper matrix. This form of iron is due to overdriving caused by a high-volume air blast in the presence of excess charcoal, which reduces the iron oxide present in the smelt. These dendrites result from the limited solubility of iron in copper below the liquidus as shown in the Cu-Fe phase diagram (Fig. 1).

In the present study, electron probe microanalysis was performed on the Timna specimen with a JEOL 733 Superprobe. All measurements were performed at 20 kV and 10 nA by use of Cu and Fe K $\alpha$  radiation. The iron dendrites are easily revealed by imaging of back-scatter electrons (Fig. 2) or Fe K $\alpha$  x-ray emission (Fig. 3). The bulk composition was determined to be 3.66 w/o Fe-95.39 w/o Cu (4.14 a/o Fe) by area scan techniques. Point counting indicated the iron dendrites to have a copper content of  $9.6 \pm 0.3$  w/o Cu (8.5 a/o Cu). Both are consistent with a melt temperature of  $1170 \pm 30$  C. Point counting in the copper matrix away from any visible second phase gave a composition of  $1.27 \pm 0.08$  w/o Fe (1.44 a/o Fe) consistent with the reduced low temperature solubility of Fe in Cu, and the presence of solid-state iron precipitates too small in size to be analyzed by the microprobe.

Studies of precipitation and aging of Cu-Fe alloys have shown that the precipitation of spherical coherent  $\gamma$ -Fe particles<sup>5</sup> occurs from the supersaturated solid solution at temperatures below the peritectic reaction temperature of  $-1095$  C. This coherency occurs because the lattice parameters of Cu ( $a_0 = 0.3615$  nm) and  $\gamma$ -Fe ( $a_0 = 0.3590$  nm) are very close in size and both possess the face-centered cubic structure.<sup>6</sup> The transformation is known to be caused by overaging<sup>7-9</sup> and/or plastic deformation's but can be suppressed by impurity additions.<sup>11,12</sup> It has been noted that precipitates smaller than a critical size will not transform<sup>5</sup> even in the presence of plastic deformation and that for aging temperatures below 800 C, no thermal treatment can transform the paramagnetic  $\gamma$ -precipitate to the  $\alpha$ -ferromagnetic form in the absence of plastic deformation, even when greatly overaged.<sup>8</sup> When the  $\gamma \rightarrow \alpha$  transformation occurs, the transformed precipitates consist of  $\{112\}_\alpha$  type twins<sup>13</sup> and have a near Kurdjumov-Sachs orientation relationship with the copper matrix.<sup>5</sup> It has also been demonstrated that the  $\gamma \rightarrow \alpha$  transformation occurs when the elastic constraints of the surrounding matrix are

---

The authors are affiliated with the Department of Metallurgy and Materials Engineering, Lehigh University, Bethlehem, PA 18015. They thank H. Moyer for performing the microprobe measurements.

removed, as through electrolytic extraction.<sup>12</sup> These observations have led to the suggestion that the  $\gamma \rightarrow \alpha$  transformation does not occur when the precipitates do not contain the crystal defects necessary to nucleate or allow the martensitic transformation to proceed.<sup>14</sup>

The morphology of the overaged precipitate has been observed in a number of the above studies. Easterling and Miekko-Oja<sup>1</sup> used replication techniques in TEM to show that aged precipitates have a cuboidal shape. Furnace-cooled specimens prepared by Boltax<sup>9</sup> contain cuboidal and star-shaped precipitates large enough to be resolved by optical microscopy. Cooke and Aschenbrenner<sup>4</sup> show similar structures for furnace-cooled alloys; however, they indicate that alloys with 2-4% Fe, remelted at 1200 C and quenched in water, are also ferromagnetic, most likely due to transformation of small residual Fe-dendrites formed during cooling, as this result is inconsistent with other studies describing solution treating and quenching experiments from below the peritectic temperature.<sup>8,9</sup>

The morphology characteristic of the overaged precipitate was observed in the current study during examination of the Timna specimen. Figure 4 is a backscattered electron image, and Fig. 5 is an Fe-K $\alpha$  x-ray image, showing the star-shaped precipitate morphology and indicating the high Fe content. As the resolution of these precipitates was poor, a thin foil was cut and ion-thinned, and the specimen was examined by TEM for better resolution and identification of these precipitates. A bright-field image (Fig. 6) obtained on a Siemens Elmiskop I 100kV electron microscope shows the star-shaped appearance of these precipitates; their common alignment indicates a possible fixed orientation relationship with the matrix. Further investigation was performed on another thin foil on a Philips EM400T operating at 120 kV. As problems were encountered with specimen thinning and as the precipitates are not uniformly distributed within the foil, it was extremely difficult to find areas with both the matrix and precipitates thin enough to produce simultaneous diffraction. One such selected area diffraction pattern is shown in Fig. 7; a dark-field image produced from one of the precipitate spots is shown in Fig. 8 and appears to illuminate only one part of the star-shaped precipitate. Tentative indexing of the pattern indicates a [011] axis for one set of spots and a [112] for the other. Both patterns appear to be FCC and to bear a fixed orientation to each other, but different from that expected from the transformed  $\gamma$ -Fe precipitates. We believe that small particles nucleated during solidification would not be aligned as is observed in Fig. 6 and would not necessarily show a simple orientation relation to the matrix that would have solidified afterwards. Therefore, we believe that the observed star-shaped precipitates were formed in the solid-state during slow cooling in the smelting furnace but maintained their FCC structure, possibly because of impurity stabilization and in the absence of plastic deformation. In any event, further study is warranted to establish the orientation relation between these precipitates and the matrix. A better understanding of the conditions under which they form might yield useful information concerning furnace conditions during smelting.

A further point deserves mention with respect to the possibly misleading statement by Cooke and Aschenbrenner<sup>4</sup> that a hand-held magnet will conclusively indicate the presence of metallic iron in a copper sample. As discussed previously, when iron precipitates in the solid state, as small coherent particles in copper-rich iron-copper alloys, it has the FCC structure and is paramagnetic. Pure Cu is diamagnetic but the solid solution of FCC c-Cu is also paramagnetic. The paramagnetic  $\gamma$ -Fe precipitates transform to ferromagnetic  $\alpha$ -Fe only under the deformation/aging conditions described previously. Third elements also have an effect on the  $\gamma - \alpha$  transformation; e.g., nickel<sup>12</sup> can completely suppress the transformation when present in amounts greater than ~5%, and similar effects have recently been observed" for the presence of Sn and Si. More work is needed in the area of other archaeologically important third elements (e.g., As, Bi, Sb) and their effect on the magnetic transformation.

#### References

1. B. Rothenberg, R. F. Tylocote, and P. J. Boydell, *Chalcolithic Copper Smelting*, Archaeometallurgy Monograph No. 1, 1981.
2. C. Milton, E. J. Dwornik, R. B. Finkelman, and P. Toulmin, "Slag from an ancient copper smelter at Timna, Israel," *J. Hist. Met. Soc.* 10: 24-33, 1976.
3. "New discoveries reveal second period of Egyptian mining," *LAMS Newsletter*, No. 1, 1980.
4. S. R. B. Cooke and S. Aschenbrenner, "The occurrence of metallic iron in ancient copper," *J. Field Archaeology* 2: 253-260, 1975.

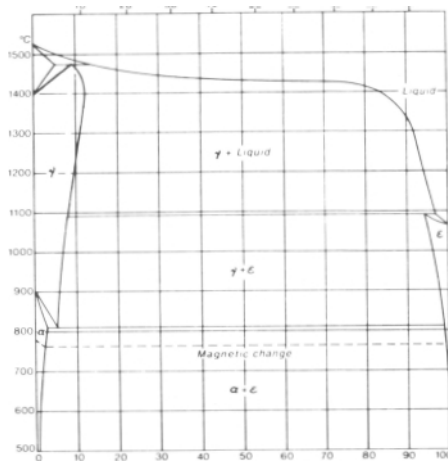


FIG. 1.--Cu-Fe phase diagram.<sup>15</sup>

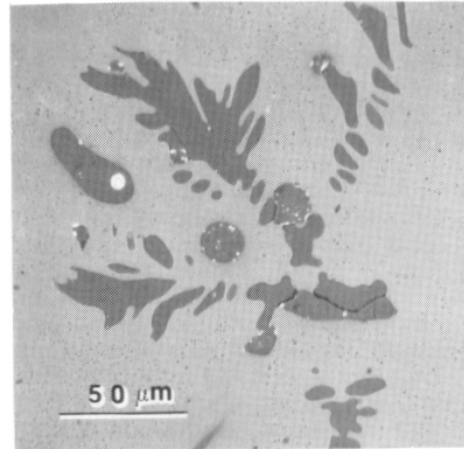


FIG. 2.--Backscatter electron image (microprobe) of iron dendrites in copper matrix.

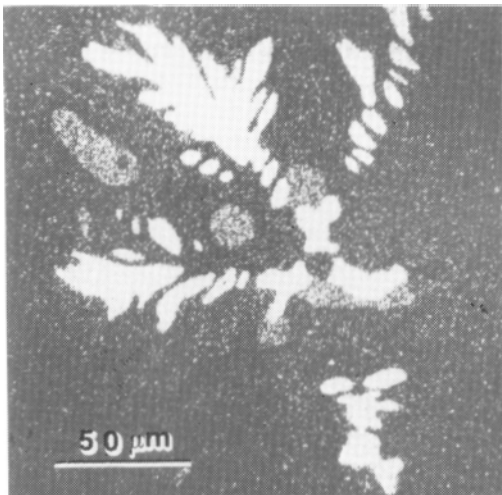


FIG. 3.--Fe K $\alpha$  x-ray image (microprobe) of iron dendrites in copper matrix.

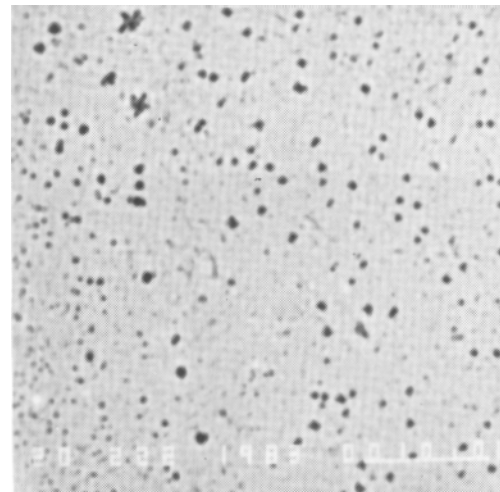


FIG. 4.--Backscatter electron image (microprobe) of iron precipitates in copper matrix.

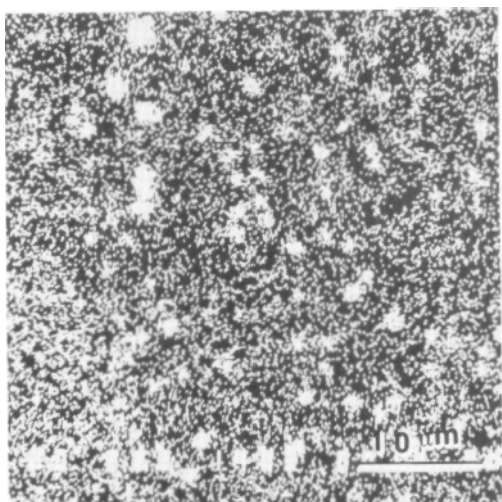


FIG. 5.--Fe K $\alpha$  x-ray image (microprobe) of iron precipitates in copper matrix.

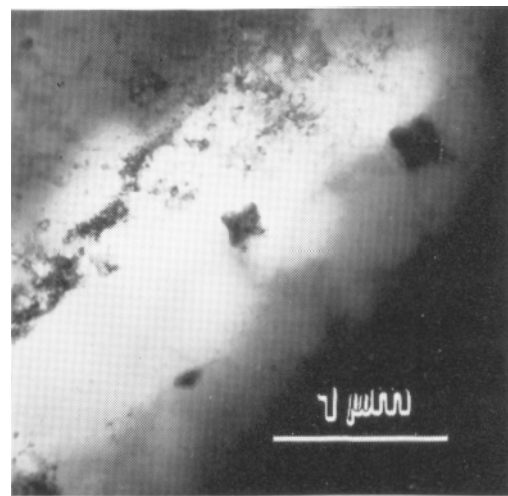


FIG. 6.--Bright-field TEM of star-shaped precipitates.

5. K. E. Easterling and G. C. Weatherly, "On the nucleation of martensite in iron precipitates," *Acta Met.* 17: 845-852, 1969.
6. J. B. Newkirk, "Mechanism of precipitation in a Cu-2.5 pct. Fe alloy," *Trans. AIME* 208: 1214-1220, 1957.
7. P. E. Cech and D. Turnbull, *J. Metals* 6: 45, 1954.
8. J. M. Denney, "Precipitation kinetics and structure in a Cu-2.4% Fe alloy," *Acta Met.* 4: 586-592, 1956.
9. A. Boltax, "Precipitation processes in copper-rich copper-iron alloys," *Trans. AIME* 218: 812-821, 1960.
10. C. S. Smith, "Structures and ferromagnetism of cold-worked copper containing iron," *Phys. Rev.* 57: 337, 1940.
11. D. Stroz, T. Panek, and H. Morawiec, "Influence of the addition of a third element to the precipitation process in Cu-Fe alloys," *Mat. Sci. and Eng.* 58: 43-53, 1983.
12. K. E. Easterling and P. R. Swann, "Nucleation of martensite in small particles," *Acta Met.* 19: 117-121, 1971.
13. R. Monzen, A. Sato, and T. Mori, "Structural changes of iron particles in a deformed and annealed Cu-Fe alloy single crystal," *Trans. Jap. Inst. Metals* 22: 65-73, 1981.
14. K. E. Easterling and H. M. Meikka-Oja, "The martensitic transformation of iron precipitates in a copper matrix," *Acta Met.* 15: 1133-1141, 1967.
15. The Cu-Fe System after *Smithells Metals Reference Book*, London: Butterworth, vol. 7; the  $\gamma/(\gamma + L)$  boundary after A. A. Bochvar, A. S. Ekatoeva, E. V. Panchenko, and Y. F. Sidokhin, *Dokl. Akad. Nauk SSSR* 174: 863-864, 1967.

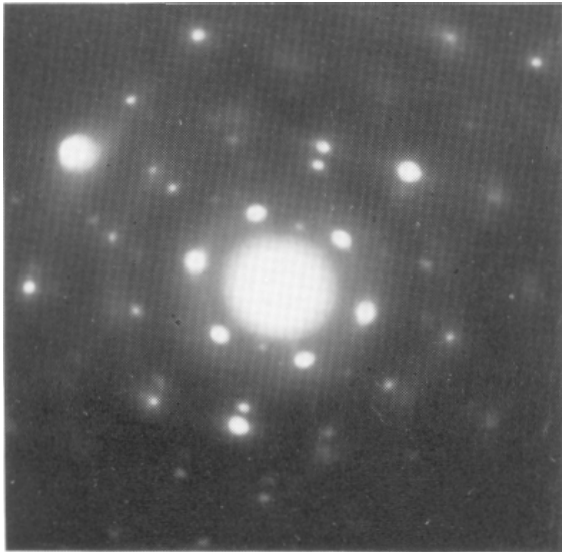


FIG. 7.--Selected-area diffraction pattern with precipitate and matrix spots superimposed.



FIG. 8.--Dark-field image (TEM) of star-shaped precipitates.